RESEARCH ARTICLE SUMMARY

EVOLUTION

Repeated co-option of HMG-box genes for sex determination in brown algae and animals

Rémy Luthringer†, Morgane Raphalen†, Carla Guerra, Sébastien Colin, Claudia Martinho, Min Zheng, Masakazu Hoshino, Yacine Badis, Agnieszka P. Lipinska, Fabian B. Haas, Josué Barrera-Redondo, Vikram Alva, Susana M. Coelho*

INTRODUCTION: The evolution of eukaryotic sex and sex-related traits has long fascinated biologists. Although core processes such as meiosis and syngamy are largely conserved, eukaryotes display a considerable diversity of sex-determination systems, raising important questions about the evolutionary dynamics of sex determination. Only a few master sex-determining genes are currently known, preventing a more comprehensive understanding of sex determination in a large phylogenetic context. Are some genes inherently better at regulating sex determination? Is there a common pathway underlying sexual differentiation across eukaryotes? These key questions remain elusive and require an analysis of sex determination that goes beyond animals and plants.

RATIONALE: In this study, we describe the discovery of the male sex-determining factor in brown algae, a major group of complex multicellular eukaryotes that are distantly related to animals and plants. In brown algae, male and female sexes are determined during the haploid phase of the life cycle by the presence of a V (male) or U (female) sex chromosome. We used classical and reverse genetics, genomics, and cell biology approaches to investigate the role of a candidate V-specific gene in determining male sex in brown algae.

RESULTS: We demonstrate that a V-specific HMG-box transcription factor, which we have named MIN (for Male INducer), is the male determinant in the model brown alga *Ectocarpus* and that its role in sex determination is conserved in kelps. HMG-box genes are also involved in sex determination in therian mammals and mating-type determination in fungi. We therefore performed a thorough investigation of the evolutionary history of eukaryotic HMG-box proteins and found that despite more than a billion years of independent evolution, animals and brown algae have independently co-opted the HMG-box for male sex determination. However, brown algae and animals exhibit differences in their sex-determination systems owing to the specific properties of the U and V sex chromosomes. Absence of *MIN* in males does not lea… sex reversal, demonstrating that the U chro… some is necessary for femaleness; thus female is not the "default" state in brown algae. Accordingly, deletion of *MIN* in male individuals carrying both the U and V chromosomes does lead to sex reversal, reinforcing the notion that the U chromosome is required for the initiation of the female developmental program.

CONCLUSION: We provide the first analysis of the molecular basis of sex determination in complex multicellular organisms beyond the animal and plant lineages, adding a new master sex-determining factor to the small list that is currently known. Our study provides evidence that the HMG-box transcription factor MIN, similar to SRY in mammals, is required for male sex determination in brown algae. Our analysis supports an independent co-option hypothesis: HMG-box genes are involved in sex determination in several eukaryotic lineages, but the specific sex-determining genes have evolved independently. Thus, the HMG-box has been recruited multiple times to play a role in sex determination across eukaryotic kingdoms, providing a fascinating example of convergent evolution over a billion-year timescale. ■

The list of author affiliations is available in the full article online.
*Corresponding author. Email: susana.coelho@tuebingen.mpg.de
†These authors contributed equally to this work.
Cite this article as: R. Luthringer *et al.*, *Science* **383**, eadk5466 (2024). DOI: 10.1126/science.adk5466

READ THE FULL ARTICLE AT
https://doi.org/10.1126/science.adk5466

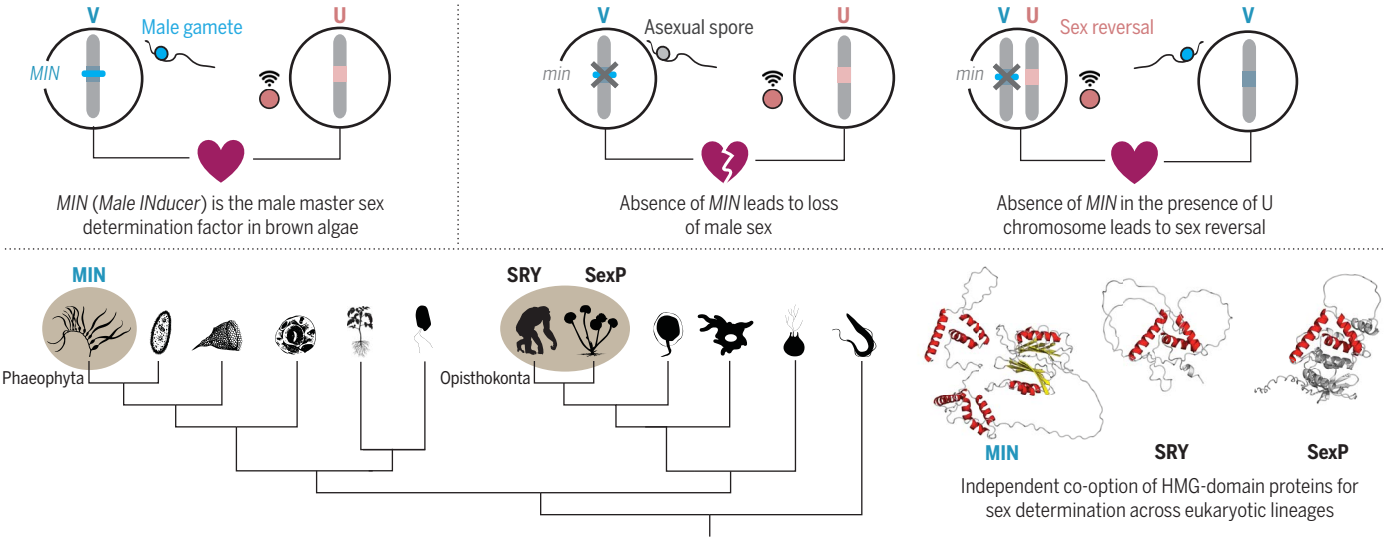

A V-specific HMG-box transcription factor, which we have named MIN (for Male INducer), is the master male determinant in brown algae, including *Ectocarpus* and the kelp *Laminaria digitata*. In the absence of a functional *MIN*, asexual "spores" are produced instead of functional sperm. The absence of *MIN* does not lead to complete sex reversal, demonstrating that the U chromosome is necessary for femaleness. Accordingly, deletion of *MIN* in individuals carrying both U and V chromosomes does lead to sex reversal. An investigation of the evolutionary history of eukaryotic HMG-box proteins revealed that despite a billion years of independent evolution, animals and phaeophytes (brown algae) have independently co-opted the HMG-box for sex determination.

RESEARCH ARTICLE

EVOLUTION

Repeated co-option of HMG-box genes for sex determination in brown algae and animals

Rémy Luthringer[1]†, Morgane Raphalen[1]†, Carla Guerra[1], Sébastien Colin[1], Claudia Martinho[1], Min Zheng[1], Masakazu Hoshino[1,2], Yacine Badis[3], Agnieszka P. Lipinska[1], Fabian B. Haas[1], Josué Barrera-Redondo[1], Vikram Alva[4], Susana M. Coelho[1]*

In many eukaryotes, genetic sex determination is not governed by XX/XY or ZW/ZZ systems but by a specialized region on the poorly studied U (female) or V (male) sex chromosomes. Previous studies have hinted at the existence of a dominant male-sex factor on the V chromosome in brown algae, a group of multicellular eukaryotes distantly related to animals and plants. The nature of this factor has remained elusive. Here, we demonstrate that an HMG-box gene acts as the male-determining factor in brown algae, mirroring the role HMG-box genes play in sex determination in animals. Over a billion-year evolutionary timeline, these lineages have independently co-opted the HMG box for male determination, representing a paradigm for evolution's ability to recurrently use the same genetic "toolkit" to accomplish similar tasks.

Three major sex chromosome systems have been identified across the diverse organisms comprising the eukaryote tree of life. The XX/XY and ZZ/ZW systems are found in diploid sexual organisms, including animals and land plants. The U/V sex system exists in eukaryotes with haploid-diploid life cycles, including the bryophytes and brown, red, and green algae (*1*). In the XX/XY system, males bear XY and females carry XX chromosomes; in the ZZ/ZW system, males have ZZ chromosomes and females ZW; and in the distinctive U/V system, females have a U chromosome and males a V chromosome (Fig. 1A). Sex-determining regions on the Y, W, V, or U chromosomes typically harbor the factor(s) responsible for triggering the male versus female sex-differentiation network. Although XY and ZW sex chromosomes have been characterized in several organisms, only a few master sex-determining factors are currently known. These include mammalian *SRY* (*2*), avian *DMRT1* (*3*), fish *DMY* (*4*, *5*), and feminizing factors such as the *–KTS* splice variant of WT1 (WT, wild-type) in mouse (*6*), *popARR17* in poplar (*7*), and *MeGI* in *Diospyros lotus* (*8*). Knowledge regarding master sex-determining factors in the U/V system is even more limited: Only one female-determining factor has been identified. This factor, present on the U chromosome of *Marchantia polymorpha*, is plant-specific (*9*). In fungi, mating-type determination is often controlled by a specialized region of the genome (the *MAT* locus), that may have properties similar to sex chromosomes (e.g., (*1*, *10*, *11*).

Despite the apparent diversity of eukaryotic sex-determination mechanisms, members of conserved gene families have been linked to sex determination in animals (*12*, *13*). For example, the *doublesex/mab-3 related* (*Dmrt*) family of transcription factors shapes sexual dimorphism in organisms as diverse as mammals, insects, and nematodes (*14*). A key member of this family, the DM domain–encoding *DMRT1* gene, is part of the mammalian sex-determination cascade, and it initiates sex determination in other vertebrate lineages (*15*, *16*). Similarly, the high-mobility group (HMG)–box domain, a small domain that binds the minor grove of DNA, is encoded by various genes involved in sex determination: the *SRY* gene that initiates male sex determination in therian mammals, various *SOX* genes involved in vertebrate sex determination, and mating-type (*MAT*) genes, which are crucial for mating type specification in fungi (*17*–*21*). Furthermore, the HMG-box domain is considerably widespread in other eukaryotic proteins, particularly in nonhistone components of chromatin and transcription factors, which often contain multiple copies that bind DNA nonspecifically (*21*). Underpinning its widespread occurrence, the most recent version of the InterPro database (v97.0; entry IPR009071) lists a significant presence of HMG-box proteins across eukaryotic species: 149 in humans, 133 in mice, 113 in zebrafish, and 8 in baker's yeast. Unlike chromatin-associated proteins, HMG-box proteins linked to sex determination typically contain a single copy of the HMG-box domain flanked by intrinsically disordered regions and bind DNA specifically. In the SRY protein of therian mammals, the HMG-box domain acts as a transcription factor that regulates other transcription factors, most importantly SOX9, eventually resulting in the development of testes (*2*, *22*, *23*). In addition to the specific binding of the SRY HMG-box domain to promoter sites, its ability to induce important conformational changes in DNA is thought to facilitate the recruitment of other factors, enabling the precise regulation of sex determination in mammals (*24*). Likewise, the HMG-box domain in the fungal MAT proteins acts as a transcription regulator, controlling the expression of genes crucial for mating-type specification and sexual reproduction (*19*).

A prominent example of the underexplored U/V sex chromosome system is found in brown algae, a group of photosynthetic multicellular organisms that thrive in coastal areas globally. As members of the stramenopiles supergroup, they have evolved independently from animals and land plants for more than a billion years (*7*), becoming the third most developmentally complex lineage on the planet (*25*). Kelps, a subgroup of brown algae, display spectacular morphologies, forming underwater forests with immense ecological importance (*26*). Most brown algal species exhibit separate sexes, which are determined by U and V sex chromosomes (*1*, *27*) (Fig. 1A). Sex is determined at meiosis (not at fertilization as in diploid XX/XY and ZW/ZZ systems), depending on whether daughter cells inherit a U or V chromosome and then develop as multicellular females or males, respectively. The level of sexual dimorphism is variable across the different brown algal species, spanning from near-isogamy (males and female gametes are very similar) to strongly oogamous (male and female gametes are strongly dimorphic) (*28*). Genetic and genomic analyses with the model brown alga *Ectocarpus sp.* (*25*, *29*) and the giant kelp *Macrocystis pyrifera* (*30*) suggest that the V sex chromosome carries a masculinizing factor, whereas the U chromosome likely harbors loci required for a complete female developmental program (*30*). Moreover, algae having both U and V chromosomes develop as males, supporting the presence of a dominant V-linked masculinizing locus (*31*, *32*). However, the identity of this sex-determining factor has remained elusive. In this study, we report the identification of the brown algal master male-determining gene, thereby revealing an important example of convergent evolution.

Identification of a candidate male-determining gene

To identify sex-determining genes, we examined genomes spanning the brown algal phylogeny and representing more than 400 million years of evolution (*33*). A single gene was

[1]Department of Algal Development and Evolution, Max Planck Institute for Biology Tübingen, 72076 Tübingen, Germany. [2]Research Center for Inland Seas, Kobe University, Kobe 658-0022, Japan. [3]Roscoff Biological Station, CNRS-Sorbonne University, Place Georges Teissier, 29680 Roscoff, France. [4]Department of Protein Evolution, Max Planck Institute for Biology Tübingen, 72076 Tübingen, Germany.
*Corresponding author. Email: susana.coelho@tuebingen.mpg.de
†These authors contributed equally to this work.

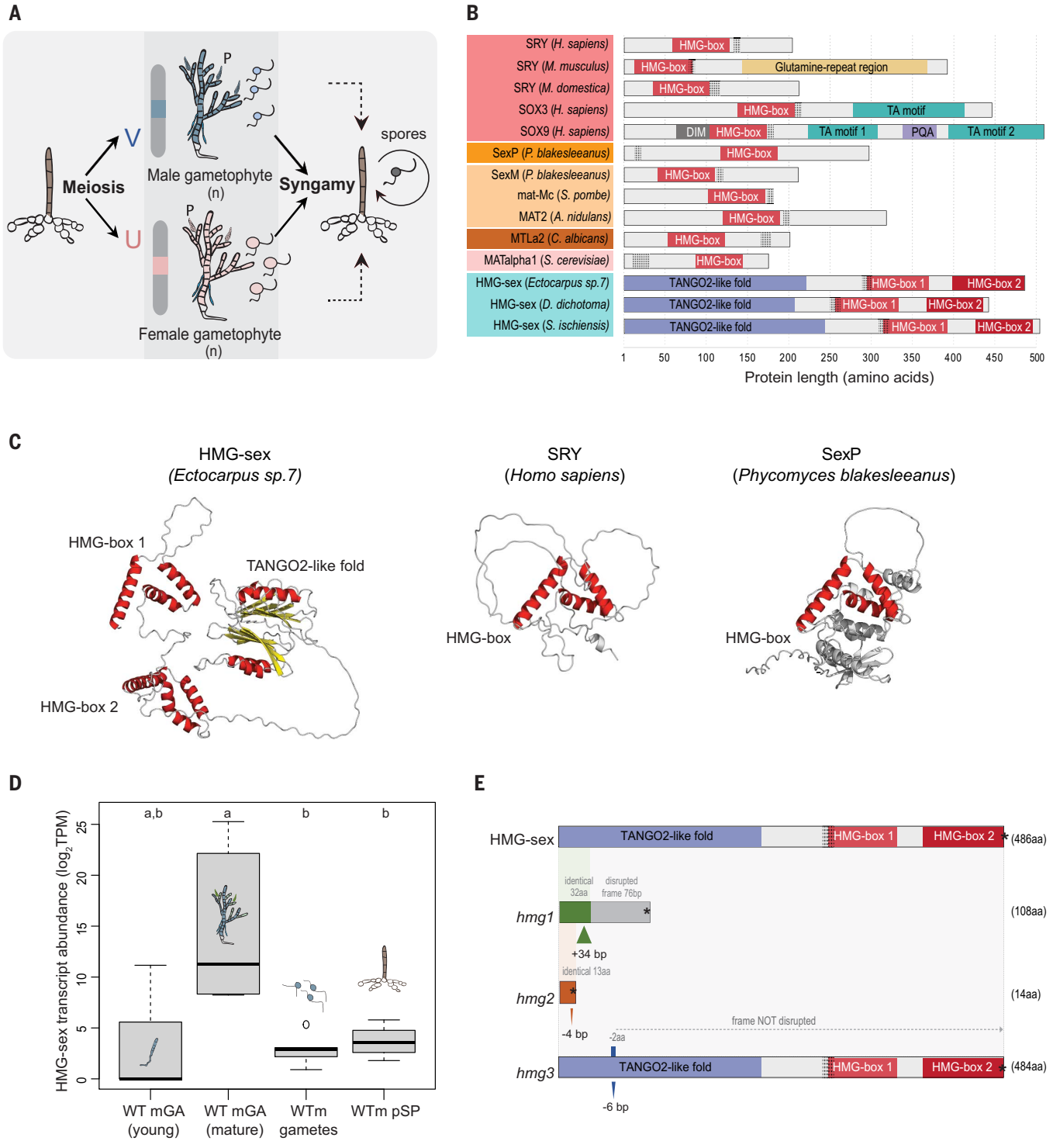

Fig. 1. An HMG-box protein coding gene located on the V-sex chromosome is a candidate master male-determining gene in brown algae. (**A**) Schematic view of the life cycle of *Ectocarpus*. Meiosis occurs in the sporophyte. The daughter cells that inherit a V sex chromosome develop into males, whereas cells that inherit a U sex chromosome develop into females. Gametes are produced in plurilocular gametangia (P), released into the seawater, and syngamy produces a sporophyte. Alternative pathways (dashed line) through parthenogenesis may occur (*96*, *97*), and gametes develop directly into parthenosporophytes. (**B**) Protein domain composition of HMG-box domain–containing proteins involved in sex determination in eukaryotes. The known domains are highlighted for each protein, and the nuclear localization signals are shown as dotted patterns within the protein. *M. domestica*: *Monodelphis domestica*. (**C**) AlphaFold2-predicted structures of HMG-sex in *Ectocarpus* alongside SRY in *Homo sapiens* and SexP in *Phycomyces blakesleeanus*. α helices are colored red and β strands yellow. (**D**) Expression level (log_2TPM) of *HMG-sex* during the life cycle of *Ectocarpus*. WT mGA, wild-type male gametophyte; WTm pSP, wild-type male parthenosporophyte. Different letters above the plot indicate significant differences (Wilcoxon test). (**E**) Scheme of WT HMG-sex protein and predicted proteins of each of the CRISPR-generated *hmg* mutants. Asterisk indicates a stop codon. aa, amino acid; bp, base pair.

V-limited in all studied species (*34*). This gene encodes a putative transcription factor featuring two HMG-box domains and a nuclear localization signal, sharing similarities with mammalian *SRY* (*2*) and fungal *MAT* genes (*11*, *19*, *35*) (Fig. 1, B and C). We will refer to this gene as *HMG-sex*. Using ColabFold (*36*, *37*), we predicted the three-dimensional (3D) structure of the *Ectocarpus sp.7* HMG-sex, revealing a canonical first HMG-box domain and a divergent second one with a large insertion (Fig. 1C and fig. S1). Additionally, HMG-sex contains an N-terminal domain with a TANGO2-like fold, characteristic of the TANGO2 family of eukaryotic and prokaryotic proteins whose functions are still largely unknown, although the human TANGO2 protein, a member of this family, has recently been implicated in lipid homeostasis (*38*). The TANGO2-like domain of HMG-sex exhibits no discernible sequence similarity to TANGO2 domains of other proteins, suggesting that it may have a distinct biological activity in brown algae.

An RNA-sequencing (RNA-seq) approach was used to investigate the expression pattern of *HMG-sex* during the *Ectocarpus* life cycle. This analysis uncovered strong up-regulation in the male mature gametophyte stage of development, when male sex is presumably determined (Fig. 1D). Although these findings suggest a role for this gene in male sex in brown algae, direct evidence is necessary to confirm that *HMG-sex* is indeed required for male sex determination.

To test this hypothesis, we generated knockout (KO) HMG-sex lines with the CRISPR-Cas system (*40*, *41*). We focused on the *HMG-sex* locus of the brown algal model *Ectocarpus sp.* (Ec-13_001750), for which genetic and genomic tools are available and whose development is well characterized (*25*, *39*, *41*–*43*). Introduction of CRISPR-Cas protein and guide RNAs targeting *HMG-sex* resulted in three independent mutant lines (*hmg1, hmg2,* and *hmg3*) (Fig. 1E and tables S1 to S4). These strains contain an additional mutation at the *APT* locus that allows selection of mutants (*39*) (table S2). *hmg1* has a +34-base pair (bp) insertion, *hmg2* has a −4-bp deletion, and *hmg3* has an in-frame deletion (−6 bp), (Fig. 1E, fig. S2, and tables S1 to S4). Mutations in *hmg1* and *hmg2* lead to a premature stop codon and a considerably disrupted predicted protein. By contrast, *hmg3* carries a −2 amino acid mutation, and the structure of the predicted protein is expected to remain unaffected (Fig. 1E and figs. S2 and S3). Consequently, *hmg3* represents a convenient additional control for specifically studying the effects of *HMG-sex* disruption.

HMG-sex is required for male gamete production

We examined the phenotype of the *hmg1*, *hmg2*, and *hmg3* mutants compared with those of control (WT and *apt*) male and female lines during various stages of the life cycle. We found no evidence for morphological feminization in the gametophytes of the three *hmg* mutants and, overall, no distinctive modification in the morphology of the *hmg* partheno-sporophytes compared with that of WT males and *apt* lines (Fig. 2A). This result is consistent with the notion that *Ectocarpus* WT male and female gametophytes display modest sexual dimorphism (*28*, *44*, *45*), with sexual differences mainly restricted to the gamete stage (*28*, *46*). We therefore tested whether the zoids produced by the *hmg* KO mutant lines behaved as fully functional male gametes.

Gamete fusion in *Ectocarpus* follows a stepwise process that begins with the attraction of male gametes to the pheromone ectocarpene produced by settled female gametes (*47*) and then proceeds with gamete recognition and cell-cell fusion (*48*, *49*). We examined the mating behavior of the *apt* and *hmg1, hmg2, and hmg3* mutant lines in response to female gametes, using high-speed video microscopy. In the absence of females, all gametes exhibit a linear swimming pattern or move in large circles (*50*), and we observed no differences in this behavior in the mutant lines as compared with the WT (fig. S4). Thus, mutations at the *HMG-sex* locus do not affect the swimming capability of the zoids.

In the presence of settled female gametes, the behavior of WT male gametes undergoes a notable change. When they sense a decrease in the sex-pheromone concentration gradient, their posterior flagellum engages in rapid, unilateral beating (*50*), causing reorientation toward the source of pheromone production. This results in a distinctive narrow circular trajectory of the gametes (*50*), leading to the formation of typical "clusters," as illustrated in Fig. 2B (see also fig. S5 and movie S1 and S2). By contrast, when *hmg1* and *hmg2* zoids were confronted with settled female gametes, their swimming pattern remained unaltered, indicating that they are unable to sense the pheromone (Fig. 2B, fig. S5, and movies S3 and S4). To confirm that the unresponsiveness of the mutant zoids was not due to decreased pheromone production by the females, we mixed WT male gametes with the same settled female gametes. Immediately, the characteristic clustering behavior of WT male gametes was observed, indicating that the female gametes were fully functional (fig. S6). Collectively, these observations suggest that although *hmg1* and *hmg2* mutant zoids exhibit a normal free-swimming pattern, they are incapable of responding to settled female gametes and therefore do not behave as fully functional males. *hmg3* (which carries a silent mutation at the *HMG* locus) behaved like WT male gametes (Fig. 2B, fig. S5, and movie S5), confirming that the lack of response to the pheromone was caused by the full disruption of the HMG-sex protein.

We evaluated fertilization success by quantifying the number of zygotes produced in controlled crosses. A substantial number of zygotes were produced in crosses involving both WT males and females, whereas no zygotes were observed when *hmg1* and *hmg2* zoids were mixed with female gametes (Fig. 2, C and D, and table S5). Conversely, crosses involving *apt* and *hmg3* mutants resulted in a zygote count comparable to that in the WT controls.

The inability of the *hmg1* and *hmg2* mutants to recognize and fuse with female gametes extended beyond their lack of attraction to the pheromone. Even when an abundance of mutant zoids was introduced, ensuring close proximity to female gametes, we observed no instances of gamete fusion (fig. S7), suggesting that mutant zoids do not "recognize" a female gamete even in close contact and are unable to engage in membrane-membrane fusion events. These observations underscore that a functional HMG-sex protein is necessary for sensing the pheromone and for recognizing and fusing with gametes of the opposite sex. Taken together, these findings indicate that HMG-sex is crucial for the manifestation of functional male characteristics in *Ectocarpus*.

The observed absence of fusion between *hmg* KO mutants and female gametes raises the possibility that *hmg* mutants may have undergone partial or even complete conversion to females. However, when we cultivated *hmg* KO zoids in isolation, we did not observe clear attraction clusters nor zygote formation (fig. S4). Furthermore, when *hmg* gametes were crossed with WT male gametes, we found neither zygotes nor evidence of attraction (fig. S8A)**.** This observation indicates that in the absence of a functional HMG-sex protein, zoids produced by mutant gametophytes become fully asexual. Although *Ectocarpus* gametes and asexual spores are morphologically indistinguishable (*51*) (see scheme in Fig. 1A), they display different swimming times before settlement. Settlement and swimming behavior of *hmg1* and *hmg2* (but not *hmg3*) zoids indeed resembled that of asexual spores (Fig. 2E and fig. S8B) and not that of male or female gametes. The absence of a functional HMG-sex, therefore, leads to the production of "demasculinized," asexual zoids in *Ectocarpus*, but does not induce sex reversal into female.

A complete sex reversion is highly unlikely in the U/V system of brown algae, given the absence of a U chromosome in males and the requirement of the U-specific region for the full expression of the female program in these organisms (*30*). This distinct feature sets it apart from XX/XY diploid systems, in which deletion of the master male-determining gene leads to phenotypic feminization (*20*). This is also unlike other haploid systems such as the

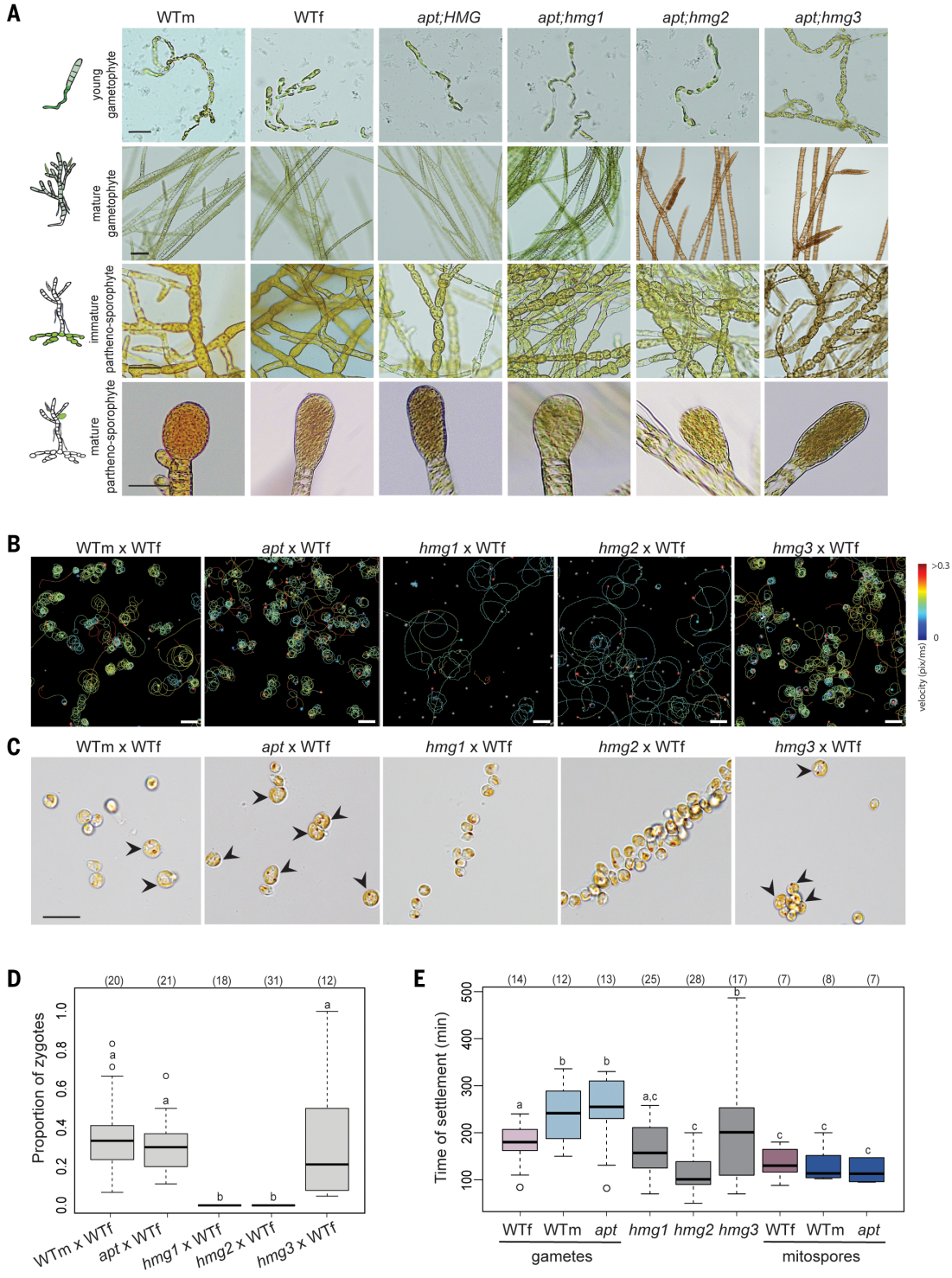

Fig. 2. Phenotype of *Ectocarpus hmg* mutants compared with WT. (**A**) Morphological phenotype of WT and *hmg* mutants during key stages of the *Ectocarpus* life cycle, schematized to the left of the photos. Scale bars, 40 μm. (**B**) A 15 s–long 2D trajectory showing the differences in swimming patterns of *Ectocarpus* WT and mutant male zoids when in contact with WT female settled gametes (see also fig. S5). Scale bars, 50 μm. (**C**) Germlings of *Ectocarpus* 24 hours after a cross. Diploid zygotes are indicated with arrowheads. Zygotes were scored by the presence of typical two eyespots, rapid cell-wall formation, and large size. By contrast, no zygotes are produced when KO *hmg1* and *hmg2* zoids are confronted with WT female gametes. Scale bar, 10 μm. (**D**) Proportion of zygotes obtained after confronting female WT gametes with different WT male and mutant strains. Between 241 and 724 germlings were scored in *n* replicates (*n* in parentheses). Different letters above the plots indicate significant differences (Wilcoxon test, $P < 0.05$) (see also table S5). (**E**) Male gametes, female gametes, and spores of *Ectocarpus* have different timing of settlement after release from the gametangia. Different letters above the plot represent significant differences ($P < 0.05$; Wilcoxon test) (see also table S7).

Volvox system, in which deletion of *VcMID* (the RWP-RK domain transcription factor determinant of sperm and egg development) results in the production of functional eggs or self-fertile hermaphrodites (*52*). This disparity may be attributed to the more complex multicellular development of *Ectocarpus* compared with that of Volvox.

It is thus possible that the lack of full sex reversal in the *Ectocarpus hmg-sex* KOs is due to the absence of the U chromosome in these individuals. To test this hypothesis, we investigated whether *HMG-sex* deletion in a genetic background containing the U chromosome would allow the U-triggered female program to be expressed. We exploited diploid gametophytes (*31*, *53*) containing both the U and V chromosome that have been shown to be phenotypically male (*31*). Two CRIPSR-Cas mutants were examined (table S3). At fertility, *UVhmg-sex* mutants released (diploid) zoids. When *UVhmg-sex* mutant zoids were confronted with WT male gametes, a large number of (triploid) zygotes were observed (fig. S9 and table S6). We therefore conclude that the presence of both the U and V chromosome in the absence of a functional HMG-sex leads to sex reversal, likely by derepression of the female (U-triggered) program. These observations imply that HMG-sex is a master regulator of male sex determination in *Ectocarpus*.

Absence of HMG-sex leads to partial transcriptome feminization

To identify pathways downstream of HMG-sex and further characterize the role of this factor in sexual differentiation, we analyzed the transcriptomes of *hmg* mutants and contrasted them with WT, *hmg3*, and *apt* background lines. Because the expression of *HMG-sex* was highest during the mature gametophyte stage (Fig. 1D), we focused on this developmental stage. Although *Ectocarpus* gametophyte morphological sexual dimorphism is almost nonexistent, male and female gametophytes express distinct transcriptomes (*44*). We used DESeq2 (*54*) to define candidate genes involved in sexual differentiation [sex-biased genes (SBGs), i.e., genes showing differential expression in WT males versus WT females]. Overall, transcriptomic patterns of SBG in mature gametophytes of all mutant samples clustered together (fig. S10). We then focused on a subset of 278 SBGs that are distinctively expressed in the presence of a functional HMG-sex (i.e., we removed SBGs that are also differentially expressed in an *apt* background), reasoning that these 278 genes are potential downstream effectors of HMG-sex (fig. S11 and table S10). Although, as we expected, transcriptomic patterns of the 278 genes in *hmg3* and *apt* resemble those of WT males, *hmg1* and *hmg2* expression profiles cluster with female WT, suggesting feminization of their expression (Fig. 3, A and B). Therefore, despite the lack of morphological effects of *HMG-sex* disruption in gametophytes (due to the absence of overall sexual dimorphism at this stage), *HMG-sex* disruption leads to gametophytic demasculinization and feminization of a subset of SBGs. Notably, these candidate effector genes are enriched in functions related to microtubule process, cell differentiation, and developmental processes (fig. S12).

HMG-sex is required for sex determination in kelps

HMG-sex is a V-linked gene across all examined brown algae with separate sexes (*34*), suggesting a conserved function in sex determination. To test this hypothesis, we generated *HMG-sex* KO mutants in the kelp *Laminaria digitata*, which diverged from *Ectocarpus* more than 100 million years ago (*33*). Sexual dimorphism in kelps is substantially more conspicuous than in *Ectocarpus* (*55*), providing an opportunity to investigate the role of HMG-sex in an organism with strong gametophyte sexual dimorphism. Two CRISPR-Cas LdHMG-sex mutant lines (Ld*hmg1*, Ld*hmg2*) were examined, both in an *apt* background (tables S3 and S11). Morphological characterization of these gametophytes revealed that they are both strongly feminized (Fig. 4, A and B). At maturity, Ld*hmg* lines did not release flagellated mobile zoids as did WT males. Instead, these lines only produced large, immobile cells resembling eggs. When male gametes were mixed with these egg-like cells, no zygotes could be observed, suggesting that they are not functional eggs. These egg-like cells were capable of parthenogenesis, which is a female-specific trait in kelps (Fig. 4C). Similarly to *Ectocarpus*, lack of a functional HMG-sex in a kelp leads to loss of maleness but not to a full sex reversal in the absence of a U chromosome (Fig. 4D). In contrast to *Ectocarpus* and consistent with the morphological sexual dimorphism

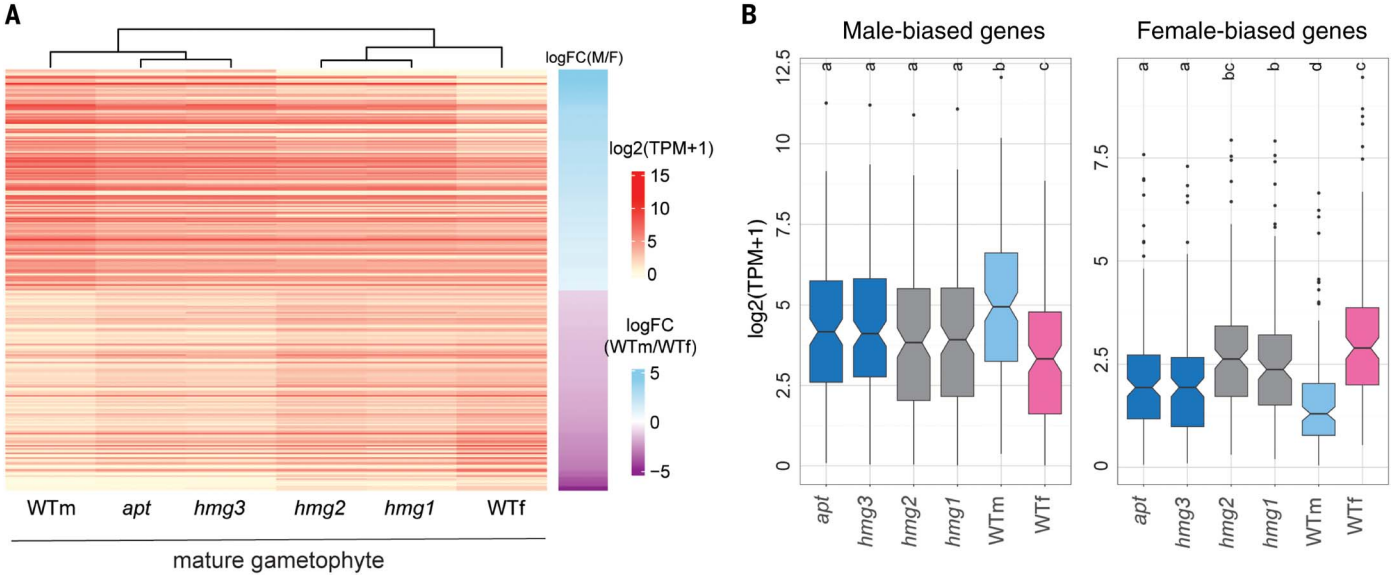

Fig. 3. Transcriptome of *Ectocarpus* HMG-sex KO gametophytes is partially feminized and demasculinized. (**A**) Hierarchical clustering of gene expression patterns in WT and mutant samples at the mature gametophyte stage of development. Heatmap was built with 287 candidate HMG-effector SBGs (see tables S8 and S9). (**B**) Transcript abundance [in $\log_2$(TPM+1)] of the 278 sex-biased genes in WT and mutant mature gametophytes. Different letters above the plots represent significant differences in expression levels (Wilcoxon rank sum test with Holm's *P*-value adjustment method).

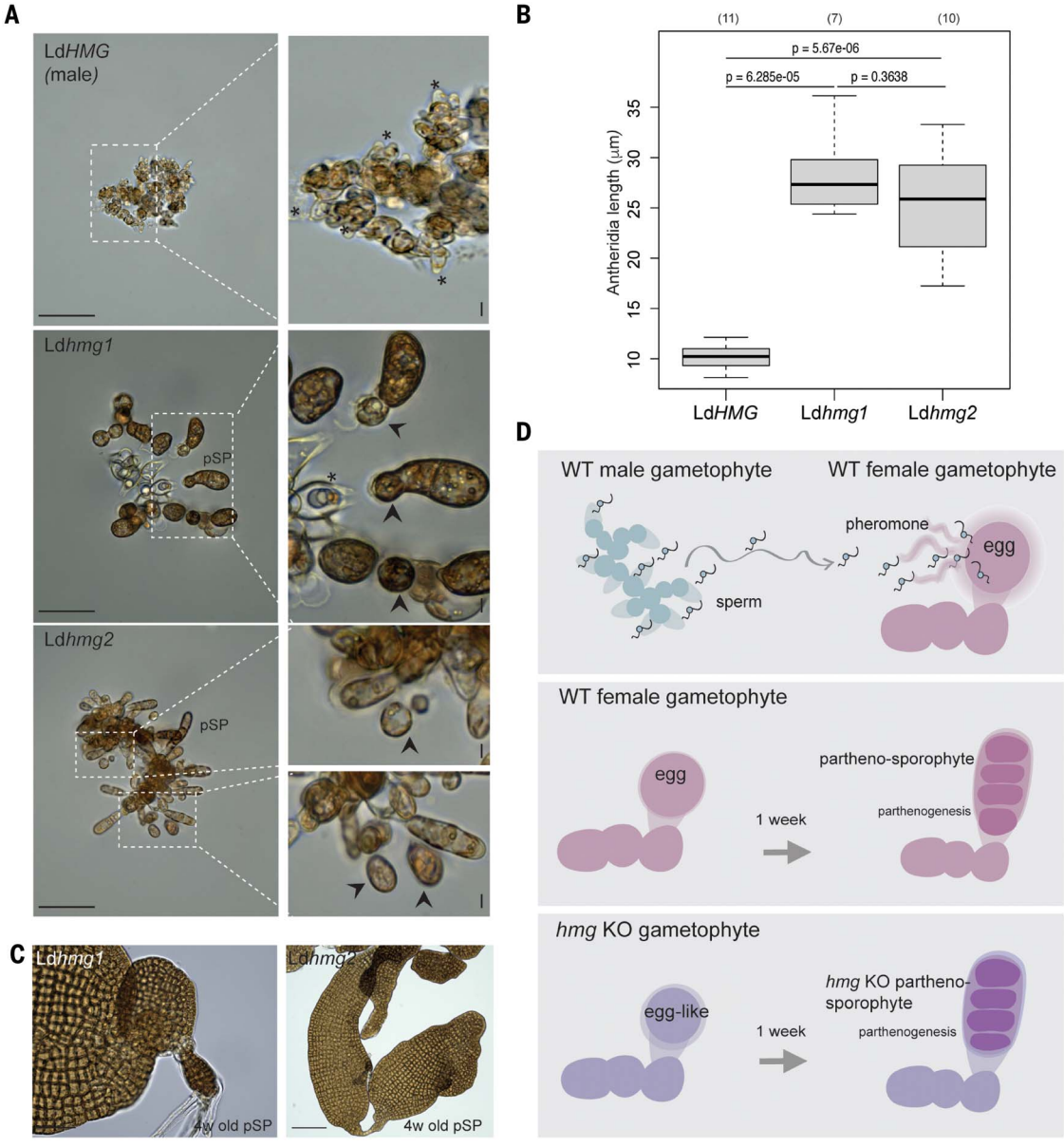

Fig. 4. HMG-sex is required for male sex determination in the kelp *L. digitata*. (**A**) Representative images of mature gametophytes of control male (Ld*HMG*) and Ld*HMG-sex* mutants (Ld*hmg1* and Ld*hmg2*). Note the pear-shaped gametangia (asterisks) where gametes are produced, which are significantly enlarged in HMG-sex mutant lines. Arrowheads highlight egg-like structures developing parthenogenetically. Scale bars, 10 μm. (**B**) Mean gametangia lengths (in μm) in *apt* lines (control) and Ld*hmg*-sex mutants. Statistical analysis was performed in R (Wilcoxon test, *P* values indicated above the plots). The number of replicates is presented in brackets. (**C**) Parthenosporophytes (pSP) developing from egg-like structures in Ld*hmg1* and Ld*hmg2* mutants. Scale bar, 50 μm. (**D**) Schematic view of development in WT and mutants. (Top) In WT males, antheridia produce biflagellate sperm cells, which are released in the media and swim toward the female eggs in response to pheromone production. (Middle) In the absence of males, WT females can reproduce by parthenogenesis, producing parthenosporophytes. (Bottom) In Ld*hmg* mutants, egg-like cells with no visible flagella are produced in enlarged gametangia. Ld*hmg* gametophytes are sterile, but the egg-like structures develop through parthenogenesis similarly to WT females.

in kelp gametophytes, mutant gametophytes were strongly feminized at the morphological level. A similar feminized phenotype was associated with silencing of HMG-sex in genetically male haploid variant lines of another kelp species (*Macrocystis pyrifera*) (*30*). Thus, HMG-sex functions as a sex-determining factor in kelps, and the partial switch to the female program in the absence of a functional HMG-sex suggests that this gene acts as a master transcription factor likely regulating the sex-differentiation pathway.

HMG-box genes function as sex determinants across eukaryotic lineages

To investigate the evolutionary origins of HMG-sex and its relationship with the HMG-box domain–containing mammalian SRY and fungal MAT proteins, we retrieved homologs of HMG-sex, SOX3, SRY, MAT, and other widespread HMG superfamily proteins, such as the FACT complex protein SSRP1 and nonhistone chromatin-associated HMGB family proteins (e.g., HMGB1), from the UniProt database (*56*). We expanded our search for homologs of HMG-sex to publicly available brown algal genomes and transcriptomes, given the limited

representation of brown algal proteins in UniProt. We then used CLANS (Cluster Analysis of Sequences) (*57*, *58*) to cluster the pooled sequences on the basis of their all-against-all pairwise sequence similarities, with an expect value (E-value) cutoff of 10^{-12}. CLANS uses the Fruchterman-Reingold force-directed layout algorithm, creating a multidimensional virtual space where protein sequences, represented as point masses, attract or repel each other based on pairwise-similarity strength (*59*). This interaction leads to evolutionarily related sequences clustering in similar areas of the map. In the resulting cluster map (Fig. 5A), SRY formed a tight cluster with various SOX proteins, with its highest similarity to SOX3, as previously reported (*60*). Whereas SOX proteins are ubiquitous in metazoans, SRY is confined to therian mammals and is thought to have evolved from SOX3 through a duplication event. Two distinct clusters, composed of MAT-associated proteins from the Ascomycota phylum and basal phyla Zoopagomycota and Mucoromycota (including SexP and SexM proteins of *Phycomyces blakesleeanus*), are closely linked to the SOX cluster. The close proximity of MAT and SOX proteins on the map suggests a shared origin from an

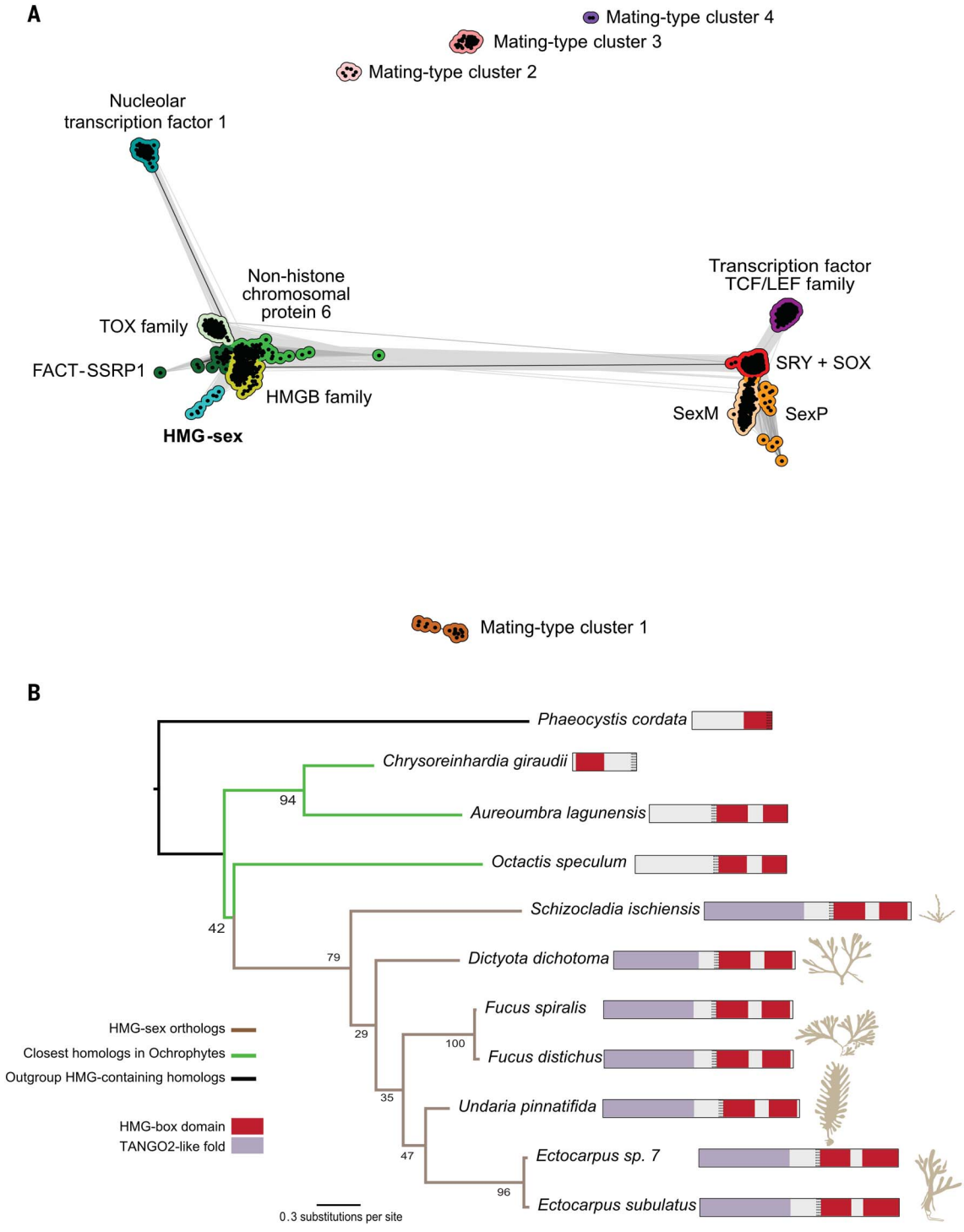

Fig. 5. HMG-box domain–containing proteins are repeatedly co-opted as sex-determining factors throughout the tree of life. (**A**) Cluster map in 2D space representing the evolutionary relationship of different sex-determining genes with HMG domains. We compiled homologs of HMG-box domain–containing proteins related to sex determination and others representative of the HMG-box domain superfamily, clustering them based on all-against-all pairwise sequence–similarity strengths. Each dot on the map represents a sequence, with sequences from the same group color-coded identically. The darkness of the connecting lines indicates the significance of sequence similarities, with darker lines representing higher significance. More details on the mating-type clusters can be found in data S1. (**B**) Maximum likelihood tree with bootstrap values displaying the evolutionary relationship and structure of HMG-sex across brown algae and other HMG-box domain–containing proteins in Ochrophyta. The nuclear localization signals are shown as dotted patterns within the protein.

ancestral protein at the root of opisthokonts. Several other well-characterized fungal MAT-associated proteins, such as MATalpha1 of *Saccharomyces cerevisiae* (mating-type cluster 2), form distinct clusters that are not linked to the SOX or the aforementioned fungal MAT clusters at the cutoff chosen for clustering, suggesting that they may represent divergent proteins. Furthermore, a cluster comprising members of the T cell factor/lymphoid enhancer factor (TCF/LEF) transcription factor family (InterPro IPR024940) involved in the Wnt signaling cascade, such as transcription factor 7, lymphoid enhancer-binding factor 1, and pangolin, is also tightly connected to the SOX cluster (Fig. 5A).

In the cluster map, HMG-sex proteins from seven distinct brown algal species, exhibiting over 35% pairwise sequence identities, form a cluster that is clearly separated from the SOX and MAT clusters. Instead, the HMG-sex cluster is linked to three distinct but tightly connected clusters, comprising the FACT complex proteins SSRP1 and Nhp6, and the HMGB family proteins (fig. S1), all of which contain representatives from a diverse range of eukaryotes. Whereas SSRP1 and Nhp6 each contain one HMG-box domain, HMGB proteins typically have two consecutive HMG-box domains like HMG-sex. Furthermore, in addition to HMG-sex, *Ectocarpus sp.* contains 12 HMG-box domain–containing proteins, with the highest sequence similarity of HMG-sex observed in proteins from the HMGB family. This suggests that HMG-sex may have evolved from the duplication and subsequent diversification of a gene encoding for an HMGB protein. However, the alternative hypothesis that it arose from the duplication of a *SSRP1-/Nhp6*-like gene cannot be fully excluded. In the cluster map, two metazoan-specific clusters of transcription factors, the TOX and nucleolar transcription factor 1 clusters, are also connected to the chromatin-associated FACT and HMGB clusters, suggesting that novel transcription factors may have arisen independently on multiple occasions from chromatin-associated HMG-box domains during the course of eukaryotic evolution. To obtain further hints about the origin of HMG-sex, we searched the EukProt database and transcriptomes of closely related sister groups of brown algae. We identified an ortholog of HMG-sex, having all three domains and exhibiting a pairwise identity of ~30%, in *Schizocladia ischiensis*. Its role in sex determination in this organism is unclear, as the life cycle cannot be completed under laboratory conditions. This search also found matches to hypothetical proteins in species of the classes Dictyochophyceae (*Octactis speculum*), and Pelagophyceae (*Aureoumbra lagunensis* and *Chrysoreinhardia giraudii*) (Fig. 5B). However, although some of these proteins have two HMG domains like HMG-sex, they do not possess an N-terminal domain of the TANGO2-like fold, suggesting that they are not orthologs of HMG-sex. Taken together, our analysis indicates that the sex-determining role of HMG-sex likely emerged in the common ancestor of brown algae, independent of opisthokonts, possibly through the duplication of an HMGB family gene. Concurrently, our data support the notion that HMG-box genes in animals and fungi, which are involved in sex determination, have a shared evolutionary origin.

Conclusions

Our experiments uncovered a male-limited *Ectocarpus* gene *HMG-sex* (Ec-13_001750), which encodes an HMG-box domain transcription factor. Loss of this gene is associated with loss of male-specific characteristics, including the ability to sense female pheromone, recognize female gametes, and produce zygotes through gamete fusion. The gametophyte transcriptome of these mutants also shows partial demasculinization and feminization. Without a functional *HMG-sex*, *Ectocarpus* gametophytes produce "demasculinized," asexual zoids. The kelp *HMG-sex* ortholog also has a male-determining role, indicating that the function of this protein has been conserved for more than 100 million years. However, the absence of HMG-sex alone is insufficient to feminize the mutants, likely owing to the lack of a U-specific region that is required to fully activate the female developmental program. Indeed, the deletion of HMG-sex in male individuals carrying both U and V chromosomes leads to sex reversal, further supporting the idea that this gene is the master male-determining gene in *Ectocarpus* and demonstrating that female is not the "default" program in this organism. We named this gene *MIN* (*MalE-INducer*) after Min, an ancient Egyptian god associated with male fertility and virility. Our investigation provides evidence that MIN, similar to SRY in mammals, is required for viable male gamete formation and male-sex determination in brown algae.

HMG-box genes play a role in sex and mating-type determination in the distantly related Opisthokonta group, which encompasses animals and fungi. Opisthokonts and brown algae diverged more than a billion years ago, and the sexes in brown algae, animals, and fungi arose independently. Thus, the similarities observed in master sex-determining factors between brown algae and opisthokonts could be attributed to either a shared ancestry or convergent evolution (*61*). Our analysis supports the independent co-option hypothesis: Even though HMG-box genes are involved in sex determination across lineages, the specific sex-determining genes have evolved independently. Thus, the HMG-box domain, likely because of its ability to induce large structural changes in DNA enabling precise control of gene regulation, has been co-opted multiple times to play a role in sex determination across eukaryotic kingdoms, providing a notable example of convergent evolution over a billion-year timescale.

Material and methods

Biological material

Table S1 describes the strains used. Ec32 is the reference genome strain (*62*). We used the male *Ectocarpus* species 7 strain Ec32, for which a reference genome is available (*62*, *63*). Strain Ec32 was previously referred to as *E. siliculosus* (*64*). However, a recent study (*65*) indicates that it belongs to a distinct, at present unnamed, species, which is referred to provisionally as *Ectocarpus* species 7 (*Ectocarpus sp. 7*). For simplicity, we use the term "*Ectocarpus*" here. The kelp *Laminaria digitata* material was collected in Santec, France, and cultured in sterilized natural seawater enriched with half-strength Provasoli solution (*66*). All strains were cultured at 14°C with a light: dark cycle of 12 hours: 12 hours (30 μmol m^{-2} s^{-1}), and daylight-type LEDs [adapted from (*67*, *68*)]. All manipulations were performed under sterile conditions in a laminar flow hood.

Generation of mutants by CRISPR-Cas

We followed the protocol described in (*39*, *40*). Our experimental system uses a single reporter gene (*UpAPT*) encoding adenine phosphoribosyl transferase (APT) and generates a resistant phenotype when algae are cultured in a medium with the toxic compound 2-fluoroadenine. Therefore, all *hmg* mutants isolated also have a mutation at the *APT* locus (table S1). Note that *apt* mutant lines have a noticeable change in their global transcriptomes so our transcriptomic comparisons were established using *apt* lines as controls. Mutations were detected by PCR amplification and Sanger sequencing. Guide RNAs and PCR primers are described in table S2.

Fertilization success and mating behavior

Reproductive success was assessed by measuring the production of zygotes in controlled experimental crosses (*69*). In brief, we mixed the same amount of male and female tissue in a suspending drop, and the proportion of gametes that succeeded in fusing (i.e., forming a zygote) was scored (table S5). Three independent parental crosses were performed. In each cross, several fields were observed and the presence of germlings (unfused gametes or zygotes) was recorded. Between 241 and 724 germlings were counted for each cross.

Mating behavior was recorded by high-speed video microscopy. Before recording, female gametes or zoids to be tested as potential pheromones producers were allowed to settle. Then, zoids were added to test their "maleness."

In the case of lack of attraction and fusion, and in order to test the "receptiveness" of female gametes, a suspension of WT male gametes was added approximately 20 min after the previous zoids suspension. All cross experiments, including the video recording, were performed at 14°C.

In order to further study the behavior of the zoids, we investigated the speed at which zoids settle after release from reproductive structures. We scored the timing of zoid settlement for the different lines studied (WT versus mutants) using an inverted microscope (Zeiss, Axiovert AX10).

Motility measurements

After allowing the female gametes to attach to the bottom surface of the imaging dish, the media was removed and replaced with a suspension of male gametes. In order to characterize the behavior of male gametes, 15-s videos at 70 frames per second (14.29 ms per frame) were acquired with an inverted microscope (Zeiss, Axiovert AX10) equipped with a global shutter cmos camera (Imaging Source, DFK37AUX250), under transmitted light illumination, with a 10x objective LD APlan (NA0.25), at the focal plane of the female gametes (circa 10 μm of depth of field).

The tracking of gamete motion was carried out with Fiji (*70*) and the plugin Trackmate (v7.11.1) (*71*). Before undertaking the tracking, images of gametes were segmented according to the following operations within Fiji: conversion of the video into a sequence of still images, image smoothing with a median filter (radius 2), autothresholding (Isodata method), binarization, holes filling within the object of interests in binary images, and watershed operation for splitting touching objects. Briefly, detected spots were filtered according to their size so that spots below 15 pixels area and above 150 pixels area (white color in the figure) were removed from the analysis. The Kalman tracker algorithm was used to track the spots, allowing a search radius of 30 pixels (circa twice the diameter of the segmented gametes) and a gap of 15 frames; and the objects with trajectories displaying a maximum distance traveled (this feature reports the distance to the furthest point of the track, with respect to the first spot in time of the track) below 25 pixels are considered as attached and nonmotile. They appear within a grey circle on the figures, whereas other spots are encircled according to the duration of their track with a jet colormap ranging values from blue (0 s) to red (15 s). Tracking conflicts caused by crossing gametes and out of focus elements were not included as they do not impact our analysis. The instantaneous velocity of the gametes is encoded in the figures with a jet colormap ranging values from blue (0.0 pixel/msec) to red (above 0.3 pixel/msec). The videos with the tracking overlay are presented as supplementary movies. Quantitative analysis of the zoid swimming path was performed as in (*48*, *50*). In brief, the distribution of the Menger curvature value K was calculated along the motion trajectory of the zoids for each tracking experiment with the different mating combinations. Menger curvature K of three points in 2D Euclidean space is the reciprocal of the radius of the distinctive circumcircle that passes through the three points (*72*). The distribution of K was measured for each position $P(x,y)$ at any timepoint $T(i)$ along tracks. The tracks were manually curated to ensure accuracy of the cell tracking, and spurious tracks were removed. For each mating experiment, a minimum of $n = 40$ tracks were analyzed. See also table S12.

DNA extraction

Genomic DNA was extracted with the OmniPep for plant kit (G-Biosciences, Cat. No. 786-397) according to the manufacturer's protocol with some modifications. Briefly, the tissue was ground to a fine powder in liquid nitrogen. 50 to 100 mg of finely ground tissue was quickly transferred to a microcentrifuge tube containing 500 μl of Lysis Buffer and carefully mixed by inverting. Then, 5 μl of Proteinase K was added to the solution and incubated at 60°C for 1 to 2 hours with periodic inversion every 15 min. After that, 200 μl of chloroform was added and a 10 min centrifugation at 14,000 g was performed. The upper phase was removed to a clean microcentrifuge tube and 50 μl of DNA Stripping Solution was added. After a 10-min incubation at 60°C, 100 μl of Precipitation Solution was added and it was incubated on ice for 15 min followed by a 10 min centrifugation at 14,000 g. The supernatant was transferred to a clean tube and 500 μl of isopropanol was added. After pelleting the genomic DNA was centrifuged at 14,000 g for 10 min, and an ethanol 75% wash was performed. Ethanol was removed and the pellet dried at room temperature, 50 μl of TE buffer was added to the pellet, and clean DNA was incubated at 60°C for 30 min. Finally, 1 μl of LongLife RNase was added for every 100 μl of TE buffer and it was incubated 30 min at 60°C. The samples were stored at −80°C until further use.

Screen for off-target mutations

The genome of the *hmg1* mutant strain was sequenced on an Illumina NextSeq 2000 platform, generating 20 Gb of sequence data, corresponding to 13.4 million 150-bp paired-end reads (accession numbers in tables S1 and S2). The sequenced reads were analyzed according to the variant calling pipeline by (*73*). Software updates were accomplished for GATK version 4.2.6.1 (*74*) and gmap-gsnap (version 2021-12-17) (*75*). The reads were mapped to the Ec32 reference genome (version v2, available at Orcae) (*76*). Potential off-target sites were predicted using Crispor (*77*) (table S3), and searches for mutations at potential off-target sites were carried out using both the table of variants and manual visualization of the genomic regions with the Jbrowse2 genome viewer (*78*).

RNA extraction and transcriptomic analysis

RNAseq was used to characterize the transcriptome of the mutant lines compared to similar stages in WT male and female lines. Biological material was grown in the conditions described above, and samples were frozen at specific stages of development. Material was flash frozen, RNA extracted using an adapted Qiagen RNAeasy procedure [as in (*13*)], and TruSeq RNA Library Prep Kit v2 was used to sequence the transcriptomes in an Illumina NextSeq 2000 platform.

RNA-seq reads from each library were used to quantify gene expression with kallisto v.0.44.0 (*79*) using 31-bp–long k-mers, 1000 bootstraps, and *Ectocarpus sp.* 7 transcriptome as reference (https://bioinformatics.psb.ugent.be/orcae/overview/EctsiV2). Transcript abundances were then summed within genes using the tximport package (*80*) to obtain the expression level for each gene in transcripts per million (TPM).

Estimates of sex-biased gene expression and pairwise differential expression between the mutants and the WT were obtained using read count matrices as input for the DESeq2 package (*54*) in R v.4.3.1. *P* values were corrected for multiple testing using Benjamini and Hochberg's algorithm in DESeq2, applying an adjusted *P*-value cutoff of 0.05 for differential expression analysis. In addition, only genes with a minimum of 2-fold change (FC) expression level between sexes were retained.

Structural model of Ectocarpus HMG-sex

Structure predictions were conducted using ColabFold (*36*), which integrates MMseqs2 for sequence similarity search and AlphaFold2 (*37*) for protein structure prediction. Given that publicly available sequence databases have limited HMG-sex sequences, many of which are incomplete, we opted for a custom-built multiple sequence alignment (MSA) as input for ColabFold. Initially, we constructed an MSA containing the HMG-sex sequence from *Ectocarpus sp. 7* and manually corrected HMG-sex sequences from various brown algal species, including *Fucus distichus*, *Fucus spiralis*, *Dictyota dichotoma*, and *Undaria pinnatifida* (*63*, *81*–*83*). The alignment was computed using MAFFT (*84*). Subsequently, this seed MSA was used to build a larger MSA by running three iterations of HHblits (*85*) against the UniRef30 database (*36*). We employed default settings when running the ColabFold pipeline using our custom MSA. Following the prediction,

the resulting models were ranked according to their pTM scores and the highest-ranking model was selected for further analysis (fig. S13). The prediction was carried out on the high-performance computer "Raven," operated by the Max Planck Computing and Data Facility in Garching, Munich, Germany. The AlphaFold2 structures of human SRY and *P. blakesleeanus* SexP shown in Fig. 1 were downloaded from the UniProt database. To assess the domain and fold composition of HMG-sex, we ran HHpred (*58*, *86*) searches against the PDB70 and ECOD70 databases and Foldseek (*87*) searches against the AlphaFold/UniProt50 v4 database, both with default settings.

Evolution of HMG-sex in the brown algae

We extracted brown algal HMG-box domain–containing proteins from publicly available genomic resources (*63*, *81*–*83*). We searched for putative orthologs of HMG-sex using OrthoFinder (*88*). We manually corrected the gene models of the HMG-sex orthologs using GenomeView (*89*) to verify that they were complete to assess its structural conservation in different species. We retrieved complete HMG-sex protein sequences for *Ectocarpus*, *Ectocarpus subulatus*, *Undaria pinnatifida*, *Fucus distichus*, *Fucus spiralis*, *Dictyota dichotoma*, and *Schizocladia ischiensis* (*63*, *81*–*83*).

To identify protein sequences for cluster analysis, we queried the UniProt database (*90*) for homologs of various HMG-box domain–containing proteins. Specifically, we focused on HMG-sex proteins from *Ectocarpus sp.* 7 and *Dictyota dichotoma*, the HMG-sex–like protein from *Schizocladia ischiensis*, and the human sex-determining region Y protein (SRY; UniProt ID: Q05066). Additionally, we searched for homologs of HMG-box domain–containing proteins implicated in the mating-type determination in fungi, including *Aspergillus nidulans* (UniProt IDs: AAP92161, G5EAT5), *Saccharomyces cerevisiae* (P0CY06), *Schizosaccharomyces pombe* (P0CY17), *Neurospora crassa* (P19392, P36981, Q10116), *Candida albicans* (Q71U11, Q9UW19), and *Phycomyces blakesleeanus* (B0F2H1, A0A167RE73). Beyond proteins involved in sex and mating-type determination, we also considered other HMG-box domain–containing proteins such as yeast nonhistone chromosomal protein 6A (P11632) and human proteins SSRP1 (Q08945), HMGB1 (P09429), SOX3 (P41225), transcription factor 7 (P36402), TOX (O94900), and nucleolar transcription factor 1 (P17480) (data S1). For the sequence similarity searches against the UniProt database, we used the HMG domains of the aforementioned proteins, predicted using InterPro (*91*), as seed sequences. Sequence similarity searches were conducted using BLAST (*90*), employing an E-value threshold of 10^{-16} and setting the "max_target_seqs" parameter to 20,000. The full-length sequences of the resulting matches were aggregated (sequences flagged as "Fragment" were removed) and subsequently filtered using MMseqs2 (*92*) to retain sequences with a maximum pairwise identity of 70% at a length coverage of at least 70%. This yielded a total of 3491 candidate sequences. These filtered sequences were then subjected to clustering analysis using CLANS (*57*, *58*). Since these proteins belong to different HMG-box domain–containing families that are highly divergent, we opted for a clustering analysis over a phylogenetic analysis to explore their evolutionary relationships. We based the clustering on all-against-all pairwise *P* values, calculated using BLAST. The clustering was performed until equilibrium was reached in a 2D space by applying a *P*-value cutoff of 10^{-12} and using the default settings in CLANS.

To further extend our search for closely related homologs of HMG-sex proteins, we also examined the EukProt database (*93*). We downloaded version 3 of EukProt and built a BLAST-searchable database using the "makeblastdb" command with default settings. BLAST searches were then conducted, also using default settings, with the HMG-sex protein sequence from *Ectocarpus* as the query. The highest bitscore hits from sister groups of brown algae were aligned with the HMG-sex orthologs using MAFFT (*84*) to reconstruct a maximum likelihood tree using RAxML (*94*). We used a protein CAT approximation and the corrected Akaike Information Criterion from RAxML to select the best empirical substitution matrix for the dataset. 100 bootstrap permutations were performed to assess the support values at each node in the tree. The HMG-box domain–containing protein of *Phaeocystis cordata* was used to root the tree. We predicted the presence of nuclear localization signals using DeepLoc 2.0 (*95*).

REFERENCES AND NOTES

1. S. M. Coelho, J. Gueno, A. P. Lipinska, J. M. Cock, J. G. Umen, UV chromosomes and haploid sexual systems. *Trends Plant Sci.* **23**, 794–807 (2018). doi: 10.1016/j.tplants.2018.06.005; pmid: 30007571
2. P. Koopman, J. Gubbay, N. Vivian, P. Goodfellow, R. Lovell-Badge, Male development of chromosomally female mice transgenic for Sry. *Nature* **351**, 117–121 (1991). doi: 10.1038/351117a0; pmid: 2030730
3. L. Beukeboom, N. Perrin, *The Evolution of Sex Determination* (Oxford Univ. Press, 2015).
4. M. Matsuda *et al*., DMY is a Y-specific DM-domain gene required for male development in the medaka fish. *Nature* **417**, 559–563 (2002). doi: 10.1038/nature751; pmid: 12037570
5. I. Nanda *et al*., A duplicated copy of DMRT1 in the sex-determining region of the Y chromosome of the medaka, Oryzias latipes. *Proc. Natl. Acad. Sci. U.S.A.* **99**, 11778–11783 (2002). doi: 10.1073/pnas.182314699; pmid: 12193652
6. E. P. Gregoire *et al*., The *-KTS* splice variant of WT1 is essential for ovarian determination in mice. *Science* **382**, 600–606 (2023). doi: 10.1126/science.add8831; pmid: 37917714
7. N. A. Müller *et al*., A single gene underlies the dynamic evolution of poplar sex determination. *Nat. Plants* **6**, 630–637 (2020). doi: 10.1038/s41477-020-0672-9; pmid: 32483326
8. T. Akagi, I. M. Henry, R. Tao, L. Comai, Plant genetics. A Y-chromosome-encoded small RNA acts as a sex determinant in persimmons. *Science* **346**, 646–650 (2014). doi: 10.1126/science.1257225; pmid: 25359977
9. M. Iwasaki *et al*., Identification of the sex-determining factor in the liverwort Marchantia polymorpha reveals unique evolution of sex chromosomes in a haploid system. *Curr. Biol.* **31**, 5522–5532.e7 (2021). doi: 10.1016/j.cub.2021.10.023; pmid: 34735792
10. S. Branco *et al*., Evolutionary strata on young mating-type chromosomes despite the lack of sexual antagonism. *Proc. Natl. Acad. Sci. U.S.A.* **114**, 7067–7072 (2017). doi: 10.1073/pnas.1701658114; pmid: 28630332
11. C. M. Hull, M.-J. Boily, J. Heitman, Sex-specific homeodomain proteins Sxi1alpha and Sxi2a coordinately regulate sexual development in Cryptococcus neoformans. *Eukaryot. Cell* **4**, 526–535 (2005). doi: 10.1128/EC.4.3.526-535.2005; pmid: 15755915
12. A. Herpin, M. Schartl, Plasticity of gene-regulatory networks controlling sex determination: Of masters, slaves, usual suspects, newcomers, and usurpators. *EMBO Rep.* **16**, 1260–1274 (2015). doi: 10.15252/embr.201540667; pmid: 26358957
13. C. S. Raymond *et al*., Evidence for evolutionary conservation of sex-determining genes. *Nature* **391**, 691–695 (1998). doi: 10.1038/35618; pmid: 9490411
14. A. Kopp, Dmrt genes in the development and evolution of sexual dimorphism. *Trends Genet.* **28**, 175–184 (2012). doi: 10.1016/j.tig.2012.02.002; pmid: 22425532
15. S. Chen *et al*., Whole-genome sequence of a flatfish provides insights into ZW sex chromosome evolution and adaptation to a benthic lifestyle. *Nat. Genet.* **46**, 253–260 (2014). doi: 10.1038/ng.2890; pmid: 24487278
16. D. Zarkower, M. W. Murphy, DMRT1: An Ancient Sexual Regulator Required for Human Gonadogenesis. *Sex Dev.* **16**, 112–125 (2022). doi: 10.1159/000518272; pmid: 34515237
17. W. Li *et al*., Identification of the mating-type (MAT) locus that controls sexual reproduction of Blastomyces dermatitidis. *Eukaryot. Cell* **12**, 109–117 (2013). doi: 10.1128/EC.00249-12; pmid: 23143684
18. A. Idnurm, F. J. Walton, A. Floyd, J. Heitman, Identification of the sex genes in an early diverged fungus. *Nature* **451**, 193–196 (2008). doi: 10.1038/nature06453; pmid: 18185588
19. J. Ait Benkhali *et al*., A network of HMG-box transcription factors regulates sexual cycle in the fungus Podospora anserina. *PLOS Genet.* **9**, e1003642 (2013). doi: 10.1371/journal.pgen.1003642; pmid: 23935511
20. S. Kurtz *et al*., Knockout of the HMG domain of the porcine SRY gene causes sex reversal in gene-edited pigs. *Proc. Natl. Acad. Sci. U.S.A.* **118**, e2008743118 (2021). doi: 10.1073/pnas.2008743118; pmid: 33443157
21. M. Štros, D. Launholt, K. D. Grasser, The HMG-box: A versatile protein domain occurring in a wide variety of DNA-binding proteins. *Cell. Mol. Life Sci.* **64**, 2590–2606 (2007). doi: 10.1007/s00018-007-7162-3; pmid: 17599239
22. C. Larney, T. L. Bailey, P. Koopman, Switching on sex: Transcriptional regulation of the testis-determining gene *Sry*. *Development* **141**, 2195–2205 (2014). doi: 10.1242/dev.107052; pmid: 24866114
23. I. Georg *et al*., Mutations of the SRY-responsive enhancer of *SOX9* are uncommon in XY gonadal dysgenesis. *Sex Dev.* **4**, 321–325 (2010). doi: 10.1159/000320142; pmid: 20838034
24. M. H. Werner, J. R. Huth, A. M. Gronenborn, G. M. Clore, Molecular basis of human 46X,Y sex reversal revealed from the three-dimensional solution structure of the human SRY-DNA complex. *Cell* **81**, 705–714 (1995). doi: 10.1016/0092-8674(95)90532-4; pmid: 7774012
25. S. M. Coelho, A. F. Peters, D. Müller, J. M. Cock, *Ectocarpus*: An evo-devo model for the brown algae. *Evodevo* **11**, 19 (2020). doi: 10.1186/s13227-020-00164-9; pmid: 32874530
26. G. Conroy, Why Earth's giant kelp forests are worth $500 billion a year. *Nature*, 18 April 2023; https://doi.org/10.1038/d41586-023-01307-3.
27. S. M. Coelho, L. Mignerot, J. M. Cock, Origin and evolution of sex-determination systems in the brown algae. *New Phytol.* **222**, 1751–1756 (2019). doi: 10.1111/nph.15694; pmid: 30667071
28. R. Luthringer *et al*., Sexual dimorphism in the brown algae. *Perspect. Phycol.* **1**, 11–25 (2015). doi: 10.1127/2198-011X/2014/0002
29. J. Cock *et al*., "Emergence of *Ectocarpus* as a model system to study the evolution of complex multicellularity in the brown algae" in *Advances in Marine Genomics*, vol. 2, *Evolutionary Transitions to Multicellular Life*, I. Ruiz-Trillo, A. Nedelcu, Eds. (Springer, 2015), pp. 153–162.
30. D. G. Müller *et al*., A partially sex-reversed giant kelp sheds light into the mechanisms of sexual differentiation in a UV

sexual system. *New Phytol.* **232**, 252–263 (2021). doi: 10.1111/nph.17582; pmid: 34166525
31. S. M. Coelho *et al*., OUROBOROS is a master regulator of the gametophyte to sporophyte life cycle transition in the brown alga *Ectocarpus*. *Proc. Natl. Acad. Sci. U.S.A.* **108**, 11518–11523 (2011). doi: 10.1073/pnas.1102274108; pmid: 21709217
32. S. Ahmed *et al*., A haploid system of sex determination in the brown alga *Ectocarpus* sp. *Curr. Biol.* **24**, 1945–1957 (2014). doi: 10.1016/j.cub.2014.07.042; pmid: 25176635
33. S.-W. Choi *et al*., Ordovician origin and subsequent diversification of the brown algae. *Curr. Biol.* **34**, 740–754.e4 (2024). doi: 10.1016/j.cub.2023.12.069; pmid: 38262417
34. A. P. Lipinska *et al*., Multiple gene movements into and out of haploid sex chromosomes. *Genome Biol.* **18**, 104 (2017). doi: 10.1186/s13059-017-1201-7; pmid: 28595587
35. D. Dooijes, M. van de Wetering, L. Knippels, H. Clevers, The Schizosaccharomyces pombe mating-type gene mat-Mc encodes a sequence-specific DNA-binding high mobility group box protein. *J. Biol. Chem.* **268**, 24813–24817 (1993). doi: 10.1016/S0021-9258(19)74537-2; pmid: 8227043
36. M. Mirdita *et al*., ColabFold: Making protein folding accessible to all. *Nat. Methods* **19**, 679–682 (2022). doi: 10.1038/s41592-022-01488-1; pmid: 35637307
37. J. Jumper *et al*., Highly accurate protein structure prediction with AlphaFold. *Nature* **596**, 583–589 (2021). doi: 10.1038/s41586-021-03819-2; pmid: 34265844
38. A. L. Lujan *et al*., Defects in lipid homeostasis reflect the function of TANGO2 in phospholipid and neutral lipid metabolism. *eLife* **12**, e85345 (2023). doi: 10.7554/eLife.85345; pmid: 36961129
39. Y. Badis *et al*., Targeted CRISPR-Cas9-based gene knockouts in the model brown alga Ectocarpus. *New Phytol.* **231**, 2077–2091 (2021). doi: 10.1111/nph.17525; pmid: 34076889
40. K. Ichihara, T. Yamazaki, S. Kawano, Genome editing using a DNA -free clustered regularly interspaced short palindromic repeats -Cas9 system in green seaweed *Ulva prolifera*. *Phycol. Res.* **70**, 50–56 (2022). doi: 10.1111/pre.12472
41. O. Godfroy *et al*., DISTAG/TBCCd1 Is Required for Basal Cell Fate Determination in *Ectocarpus*. *Plant Cell* **29**, 3102–3122 (2017). doi: 10.1105/tpc.17.00440; pmid: 29208703
42. O. Godfroy *et al*., The *baseless* mutant links protein phosphatase 2A with basal cell identity in the brown alga *Ectocarpus*. *Development* **150**, dev201283 (2023). doi: 10.1242/dev.201283; pmid: 36786333
43. N. Macaisne *et al*., The *Ectocarpus IMMEDIATE UPRIGHT* gene encodes a member of a novel family of cysteine-rich proteins with an unusual distribution across the eukaryotes. *Development* **144**, 409–418 (2017). pmid: 28049657
44. A. Lipinska *et al*., Sexual dimorphism and the evolution of sex-biased gene expression in the brown alga *Ectocarpus*. *Mol. Biol. Evol.* **32**, 1581–1597 (2015). doi: 10.1093/molbev/msv049; pmid: 25725430
45. G. G. Cossard *et al*., Selection drives convergent gene expression changes during transitions to co-sexuality in haploid sexual systems. *Nat. Ecol. Evol.* **6**, 579–589 (2022). doi: 10.1038/s41559-022-01692-4; pmid: 35314785
46. J. Gueno *et al*., Chromatin landscape associated with sexual differentiation in a UV sex determination system. *Nucleic Acids Res.* **50**, 3307–3322 (2022). doi: 10.1093/nar/gkac145; pmid: 35253891
47. I. Maier, "Brown algal pheromones" in *Progress in Phycological Research* vol. 11, D. J. Chapman, F. E. Round, Eds. (Biopress Ltd., 1995), pp. 51–102.
48. A. Geller, D. G. Müller, Analysis of the flagellar beat pattern of male *Ectocarpus siliculosus* gametes (Phaeophyta) in relation to chemotactic stimulation by female cells. *J. Exp. Biol.* **92**, 53–66 (1981). doi: 10.1242/jeb.92.1.53
49. I. Maier, C. Schmid, An immunofluorescence study on lectin binding sites in gametes of Ectocarpus siliculosus (Ectocarpales, Phaeophyceae). *Phycol. Res.* **43**, 33–42 (2006). doi: 10.1111/j.1440-1835.1995.tb00003.x
50. N. Kinoshita *et al*., Flagellar waveforms of gametes in the brown alga *Ectocarpus siliculosus*. *Eur. J. Phycol.* **51**, 139–148 (2016). doi: 10.1080/09670262.2015.1109144
51. B. Charrier *et al*., Development and physiology of the brown alga *Ectocarpus siliculosus*: Two centuries of research. *New Phytol.* **177**, 319–332 (2008). doi: 10.1111/j.1469-8137.2007.02304.x; pmid: 18181960
52. S. Geng, P. De Hoff, J. G. Umen, Evolution of sexes from an ancestral mating-type specification pathway. *PLOS Biol.* **12**, e1001904 (2014). doi: 10.1371/journal.pbio.1001904; pmid: 25003332
53. S. M. Coelho *et al*., Genetic regulation of life cycle transitions in the brown alga *Ectocarpus*. *Plant Signal. Behav.* **6**, 1858–1860 (2011). doi: 10.4161/psb.6.11.17737; pmid: 22067105
54. M. I. Love, W. Huber, S. Anders, Moderated estimation of fold change and dispersion for RNA-seq data with DESeq2. *Genome Biol.* **15**, 550 (2014). doi: 10.1186/s13059-014-0550-8; pmid: 25516281
55. S. Heesch *et al*., Evolution of life cycles and reproductive traits: Insights from the brown algae. *J. Evol. Biol.* **34**, 992–1009 (2021). doi: 10.1111/jeb.13880; pmid: 34096650
56. UniProt Consortium, UniProt: The Universal Protein Knowledge base in 2023. *Nucleic Acids Res.* **51** (D1), D523–D531 (2023). doi: 10.1093/nar/gkac1052; pmid: 36408920
57. T. Frickey, A. Lupas, CLANS: A Java application for visualizing protein families based on pairwise similarity. *Bioinformatics* **20**, 3702–3704 (2004). doi: 10.1093/bioinformatics/bth444; pmid: 15284097
58. L. Zimmermann *et al*., A Completely Reimplemented MPI Bioinformatics Toolkit with a New HHpred Server at its Core. *J. Mol. Biol.* **430**, 2237–2243 (2018). doi: 10.1016/j.jmb.2017.12.007; pmid: 29258817
59. T. M. J. Fruchterman, E. M. Reingold, Graph drawing by force-directed placement. *Softw. Pract. Exper.* **21**, 1129–1164 (1991). doi: 10.1002/spe.4380211102
60. M. Stevanović, R. Lovell-Badge, J. Collignon, P. N. Goodfellow, *SOX3* is an X-linked gene related to *SRY*. *Hum. Mol. Genet.* **2**, 2013–2018 (1993). doi: 10.1093/hmg/2.12.2013; pmid: 8111369
61. J. A. Marshall Graves, C. L. Peichel, Are homologies in vertebrate sex determination due to shared ancestry or to limited options? *Genome Biol.* **11**, 205 (2010). doi: 10.1186/gb-2010-11-4-205; pmid: 20441602
62. J. M. Cock *et al*., The *Ectocarpus* genome and the independent evolution of multicellularity in brown algae. *Nature* **465**, 617–621 (2010). doi: 10.1038/nature09016; pmid: 20520714
63. A. Cormier *et al*., Re-annotation, improved large-scale assembly and establishment of a catalogue of noncoding loci for the genome of the model brown alga *Ectocarpus*. *New Phytol.* **214**, 219–232 (2017). doi: 10.1111/nph.14321; pmid: 27870061
64. A. F. Peters, D. Marie, D. Scornet, B. Kloareg, J. Mark Cock, Proposal of *Ectocarpus Siliculosus* (Ectocarpales, Phaeophyceae) as a Model Organism for Brown Algal Genetics And Genomics1,2. *J. Phycol.* **40**, 1079–1088 (2004). doi: 10.1111/j.1529-8817.2004.04058.x
65. A. E. Montecinos *et al*., Species delimitation and phylogeographic analyses in the Ectocarpus subgroup siliculosi (Ectocarpales, Phaeophyceae). *J. Phycol.* **53**, 17–31 (2017). doi: 10.1111/jpy.12452; pmid: 27454456
66. R. Starr, J. Zeikus, UTEX—The Culture Collection of Algae at The University Of Texas at Austin 1993 List Of Cultures. *J. Phycol.* **29**, 1–106 (2004). doi: 10.1111/j.0022-3646.1993.00001.x
67. S. M. Coelho *et al*., How to cultivate *Ectocarpus*. *Cold Spring Harb. Protoc.* **2012**, 258–261 (2012). doi: 10.1101/pdb.prot067934; pmid: 22301662
68. A. F. Peters *et al*., Life-cycle-generation-specific developmental processes are modified in the immediate upright mutant of the brown alga *Ectocarpus siliculosus*. *Development* **135**, 1503–1512 (2008). doi: 10.1242/dev.016303; pmid: 18339673
69. S. M. Coelho *et al*., Genetic crosses between *Ectocarpus* strains. *Cold Spring Harb. Protoc.* **2012**, 262–265 (2012). doi: 10.1101/pdb.prot067942; pmid: 22301663
70. J. Schindelin *et al*., Fiji: An open-source platform for biological-image analysis. *Nat. Methods* **9**, 676–682 (2012). doi: 10.1038/nmeth.2019; pmid: 22743772
71. D. Ershov *et al*., TrackMate 7: Integrating state-of-the-art segmentation algorithms into tracking pipelines. *Nat. Methods* **19**, 829–832 (2022). doi: 10.1038/s41592-022-01507-1; pmid: 35654950
72. M. Berger, "Menger curvature" in *Geometry*, vol. 1 (Springer-Verlag, 1987), p. 273.
73. F. B. Haas *et al*., Single Nucleotide Polymorphism Charting of *P. patens* Reveals Accumulation of Somatic Mutations During *in vitro* Culture on the Scale of Natural Variation by Selfing. *Front. Plant Sci.* **11**, 813 (2020). doi: 10.3389/fpls.2020.00813; pmid: 32733496
74. A. McKenna *et al*., The Genome Analysis Toolkit: A MapReduce framework for analyzing next-generation DNA sequencing data. *Genome Res.* **20**, 1297–1303 (2010). doi: 10.1101/gr.107524.110; pmid: 20644199
75. T. D. Wu, S. Nacu, Fast and SNP-tolerant detection of complex variants and splicing in short reads. *Bioinformatics* **26**, 873–881 (2010). doi: 10.1093/bioinformatics/btq057; pmid: 20147302
76. L. Sterck, K. Billiau, T. Abeel, P. Rouzé, Y. Van de Peer, ORCAE: Online resource for community annotation of eukaryotes. *Nat. Methods* **9**, 1041–1041 (2012). doi: 10.1038/nmeth.2242; pmid: 23132114
77. M. Haeussler *et al*., Evaluation of off-target and on-target scoring algorithms and integration into the guide RNA selection tool CRISPOR. *Genome Biol.* **17**, 148 (2016). doi: 10.1186/s13059-016-1012-2; pmid: 27380939
78. C. Diesh *et al*., JBrowse 2: A modular genome browser with views of synteny and structural variation. *Genome Biol.* **24**, 74 (2023). doi: 10.1186/s13059-023-02914-z; pmid: 37069644
79. N. L. Bray, H. Pimentel, P. Melsted, L. Pachter, Near-optimal probabilistic RNA-seq quantification. *Nat. Biotechnol.* **34**, 525–527 (2016). doi: 10.1038/nbt.3519; pmid: 27043002
80. C. Soneson, M. I. Love, M. D. Robinson, Differential analyses for RNA-seq: Transcript-level estimates improve gene-level inferences. *F1000Research* **4**, 1521 (2015). doi: 10.12688/f1000research.7563.1; pmid: 26925227
81. K. A. Bogaert, T. Beeckman, O. De Clerck, Two-step cell polarization in algal zygotes. *Nat. Plants* **3**, 16221 (2017). doi: 10.1038/nplants.2016.221; pmid: 28112726
82. T. Yamagishi, D. G. Müller, H. Kawai, Comparative transcriptome analysis of *Discosporangium mesarthrocarpum* (Phaeophyceae), *Schizocladia ischiensis* (Schizocladiophyceae), and *Phaeothamnion confervicola* (Phaeothamniophyceae), with special reference to cell wall-related genes. *J. Phycol.* **50**, 543–551 (2014). doi: 10.1111/jpy.12190; pmid: 26988326
83. W. J. Hatchett *et al*., Evolutionary dynamics of sex-biased gene expression in a young XY system: Insights from the brown alga genus *Fucus*. *New Phytol.* **238**, 422–437 (2023). doi: 10.1111/nph.18710; pmid: 36597732
84. K. Katoh, K. Misawa, K. Kuma, T. Miyata, MAFFT: A novel method for rapid multiple sequence alignment based on fast Fourier transform. *Nucleic Acids Res.* **30**, 3059–3066 (2002). doi: 10.1093/nar/gkf436; pmid: 12136088
85. M. Remmert, A. Biegert, A. Hauser, J. Söding, HHblits: Lightning-fast iterative protein sequence searching by HMM-HMM alignment. *Nat. Methods* **9**, 173–175 (2011). doi: 10.1038/nmeth.1818; pmid: 22198341
86. M. Steinegger *et al*., HH-suite3 for fast remote homology detection and deep protein annotation. *BMC Bioinformatics* **20**, 473 (2019). doi: 10.1186/s12859-019-3019-7; pmid: 31521110
87. M. van Kempen *et al*., Fast and accurate protein structure search with Foldseek. *Nat. Biotechnol.* **42**, 243–246 (2024). doi: 10.1038/s41587-023-01773-0; pmid: 37156916
88. D. M. Emms, S. Kelly, OrthoFinder: Solving fundamental biases in whole genome comparisons dramatically improves orthogroup inference accuracy. *Genome Biol.* **16**, 157 (2015). doi: 10.1186/s13059-015-0721-2; pmid: 26243257
89. T. Abeel, T. Van Parys, Y. Saeys, J. Galagan, Y. Van de Peer, GenomeView: A next-generation genome browser. *Nucleic Acids Res.* **40**, e12–e12 (2012). doi: 10.1093/nar/gkr995; pmid: 22102585
90. R. Zaru, S. Orchard, UniProt Consortium, UniProt Tools: BLAST, Align, Peptide Search, and ID Mapping. *Curr. Protoc.* **3**, e697 (2023). doi: 10.1002/cpz1.697; pmid: 36943033
91. E. Quevillon *et al*., InterProScan: Protein domains identifier. *Nucleic Acids Res.* **33** (Web Server), W116–W120 (2005). doi: 10.1093/nar/gki442; pmid: 15980438
92. M. Steinegger, J. Söding, MMseqs2 enables sensitive protein sequence searching for the analysis of massive data sets. *Nat. Biotechnol.* **35**, 1026–1028 (2017). doi: 10.1038/nbt.3988; pmid: 29035372
93. D. J. Richter *et al*., EukProt: A database of genome-scale predicted proteins across the diversity of eukaryotes. *Peer Community J.* **2**, e56 (2022). doi: 10.24072/pcjournal.173
94. A. Stamatakis, RAxML version 8: A tool for phylogenetic analysis and post-analysis of large phylogenies. *Bioinformatics* **30**, 1312–1313 (2014). doi: 10.1093/bioinformatics/btu033; pmid: 24451623
95. V. Thumuluri, J. J. Almagro Armenteros, A. R. Johansen, H. Nielsen, O. Winther, DeepLoc 2.0: Multi-label subcellular localization prediction using protein language models. *Nucleic Acids Res.* **50** (W1), W228–W234 (2022). doi: 10.1093/nar/gkac278; pmid: 35489069
96. L. Mignerot, K. Avia, R. Luthringer, A. P. Lipinska, A. F. Peters, J. M. Cock, S. M. Coelho, A key role for sex chromosomes in the regulation of parthenogenesis in the brown alga *Ectocarpus*. *PLOS Genet.* **15**, e1008211 (2019). doi: 10.1371/journal.pgen.1008211; pmid: 31194744

97. J. H. Bothwell, D. Marie, A. F. Peters, J. M. Cock, S. M. Coelho, Role of endoreduplication and apomeiosis during parthenogenetic reproduction in the model brown alga *Ectocarpus*. *New Phytol.* **188**, 111–121 (2010). doi: 10.1111/j.1469-8137.2010.03357.x; pmid: 20618911
98. H. Fabian, Single nucleotide polymorphism charting of P. patens reveals accumulation of somatic mutations during in vitro culture on the scale of natural variation by selfing. (2020). doi: 10.5281/ZENODO.10563846

ACKNOWLEDGMENTS

We thank A. Henschen for the help with DNA extractions and A. Belkacemi and D. Koch for assistance with algal cultures. D. Liesner shared HMG and APT sequences from *Laminaria pallida*. **Funding:** This research was supported by the Max Planck Society, European Research Council grant 864038 (S.M.C.), the Moore Foundation (S.M.C.), and the Alexander von Humboldt Foundation (J.B.-R.). **Author contributions:** Conceptualization: S.M.C. Methodology: S.M.C., R.L., M.H., S.C., Y.B., M.R., C.M., and V.A. Investigation: M.R., R.L., C.G., M.H., S.C., A.P.L., F.B.H., J.B.-R., V.A., M.Z., and C.M. Visualization: S.M.C., V.A., and J.B.-R. Funding acquisition: S.M.C. Project conceptualization and administration: S.M.C. Supervision: S.M.C., V.A., and J.B.-R. Writing – original draft: S.M.C., R.L., J.B.-R., and V.A. Writing – review and editing: S.M.C. **Competing interests:** The authors declare that they have no competing interests. **Data and materials availability:** All data are available at the NCBI BioProject PRJNA1022600 and in the main text or the supplementary materials; accession codes are listed in tables S3 and S4. Code for the SNP pipeline is available at Zenodo (*98*).

SUPPLEMENTARY MATERIALS

science.org/doi/10.1126/science.adk5466
Figs. S1 to S13
Tables S1 to S12
Movies S1 to S5
MDAR Reproducibility Checklist
Data S1

Submitted 10 October 2023; accepted 31 January 2024
10.1126/science.adk5466